

Chaotic hidden attractor in a fractional order system modelling the interaction between dark matter and dark energy

Marius-F. Danca*

STAR-UBB Institute, Babes-Bolyai University

400084 Cluj-Napoca, Romania

Email: m.f.danca@gmail.com

November 27, 2023

Abstract

In this paper the dynamics of a fractional order system modelling the interaction between dark matter and dark energy is analytically and numerically studied. It is shown for the first time that systems modelling the interaction between dark matter and dark energy, chaotic hidden attractors can be present. The chaotic attractor co-exists with two asymptotically stable equilibria. Equilibria of the linearized system exhibit a center-like behavior. The numerical integration is done by means of the Adams-Bashforth-Moulton scheme and the finite Lyapunov exponents are numerically determined with a dedicated Matlab code. The 3D representation of the chaotic hidden attractor reveals the fact it is not connected with the equilibria, being “hidden” somewhere in the considered phase space.

keyword Fractional calculus; Caputo fractional derivative; Hidden chaotic attractor

1 Introduction

The interaction between dark matter and dark energy, which affects the cosmic structures, is one of not completely solved problems in cosmology and has been studied extensively [1]. Our universe, which continues to expand, consists not only of matter but also dark matter and dark energy. Today, we know that our universe is composed of about 68.3 dark energy, 26.8 dark matter and 4.9 regular matter according to Planck data [2] (detailed references on interaction between dark energy and dark matter can be found in [1] and [2]). In [2] is introduced a coupled system of Integer Order (IO) modeling the Interaction between Dark

*Corresponding author

Matter and Dark Energy (IDMDE) (see also [3] where the coupling interactions among dark energy, dark matter, and matter are modeled by three coupled logistic models)

$$\begin{aligned}\dot{x}_1 &= x_2 x_3 - x_1, \\ \dot{x}_2 &= (x_3 - p)x_1 - x_2, \\ \dot{x}_3 &= 1 - x_1 x_2,\end{aligned}\tag{1}$$

where p is a real parameter considered positive in this paper. Despite his simple form, in [2] it is shown that the system has a clear physical sense and the numerical study realized reveals that for $p = 3.46$, the system behaves chaotically.

Without being one of the algebraically simplest chaotic systems (see [4, 5]), its rich potential chaotic behavior represented the motivation to go beyond the obtained results in [2] and to consider the Fractional Order (FO) form of the IO system (1), study which reveal more interesting dynamics such as the existence of hidden attractors which to our knowledge it's a novelty and, therefore, could influence the theory of interaction coupling between dark matter and dark energy and help to understand the observed acceleration of cosmic expansion.

The concept of non-integer or FO derivatives dates back to the beginning of the theory of differential calculus, while the development of fractional calculus dates since the work of Euler, Liouville, Riemann, Letnikov [6, 7]. The fractional calculus is as old as the integer-order one, but with application exclusively in mathematics. Fractional calculus can be applied to real life problems and, therefore, fractional derivatives and integrals are useful in engineering and mathematics, being helpful for scientists and researchers working with real-life applications (see, e.g., [2, 8]). One of the famous operator of FO is Caputo's fractional derivative, proposed by Caputo in 1967 and utilized in this paper. Fractional derivatives model phenomena which takes account of interactions within the past (equation with "memory"). Moreover, fractional derivatives describe nonlocality in space and time. Basic aspects of the theory of fractional differential equations can be found in the monograph [9], or in [10]. Also see [11] for a review of definitions of fractional derivatives and other operators. One of the usually utilized numerical schemes for integration of continuous systems of FO which is used in this paper is the Adams-Bashforth-Moulton predictor-corrector method [12].

Not only fractional differential equations aroused the interest of scientists, but also fractional difference equations, one of the first definition of a fractional difference operator dating from 1974 [45] (several references on fractional differences can be found e.g. in [13]). Initial value problems for fractional differences are described in [14], while applications can be found in [15–18].

Both for continuous time and discrete time systems, Caputo's differential operator allows the formulation of initial conditions for initial-value problems in traditional form, as for integer-order initial-value problems, reason why it was chosen in this paper.

It is to note that the dynamics of many real systems are better described non-integer derivatives which incorporate memory and hereditary features of systems. So, in order to accurately describe these systems, the fractional-order differential equations have been introduced. In chaos theory, it has been observed that chaos occurs in dynamical systems of order 3 or more. With the introduction of fractional-order systems, it was shown that chaos in systems FO systems exist even the total order is less than 3.

Recently a new term *hidden attractor* has been introduced in IO systems and, later, in FO systems (see e.g. [19] or [20], one of the first works on this subject). If the attraction basin of a considered attractor intersects with any open neighborhoods of an equilibrium, the attractor is called *self-excited*, otherwise, it is called *hidden*. Usually, the self-excited attractors are numerically derived from unstable equilibria, while hidden attractors are difficult to be localized, because their attraction basins have no relation with small neighborhoods of any equilibria. References on systems type where hidden attractors appear are presented in [21]. The importance of hidden attractors is underlined for example by the hidden oscillations which might occur at aircrafts and launchers control systems [22].

The paper focus on showing numerically that a FO variant of an existing IO system modelling the interaction between dark matter and dark energy, can present hidden attractors. For this purpose, it is proved numerically and via Matignon's criterion, that equilibria are asymptotically stable for all fractional order $q \in (0, 1)$ and parameter q . Next, based on the existence of local Lyapunov Exponents and their three-dimensionally plot, it is shown that the attracting set, reached by trajectories starting from an appropriate basin, is chaotic. The LEs are determined with a dedicated Matlab code. Since all considered trajectories attracted by the chaotic attractor do not cross relatively small neighborhoods of the stable equilibria, the attractor verifies the definition of a hidden attractor. Also, it is shown that, considering too short time integration intervals (approach used in several works), could lead to false results, i.e., chaotic transients, like in the considered system. A FO variant of divergence for the considered system is presented as an interesting approach of stability.

The paper is organized as follows: Section 2 introduces the FO variant of the IDMDE system; Section 3 presents equilibria of the FO system and their stability; Section 4 deals with Lyapunov exponents; In Section 5 the chaotic hidden attractor is analyzed and the Conclusion section ends the paper.

2 IDMDE system of FO

We consider in this paper the commensurate FO variant of the IDMDE system (1) in Caputo's sense, modeled by the following FO initial value problem

$$D_*^q x(t) = f(x(t)), \quad x(0) = x_0, \quad (2)$$

where $x = (x_1, x_2, x_3)$, and $f : \mathbb{R}^3 \rightarrow \mathbb{R}^3$ is the vector-valued function

$$f(x) = \begin{pmatrix} x_2 x_3 - x_1 \\ (x_3 - p)x_1 - x_2 \\ 1 - x_1 x_2 \end{pmatrix},$$

and D_*^q stands as Caputo's derivative with starting point 0, of order q being defined as follows

$$D_*^q x = \frac{1}{\Gamma[q] - q} \int_0^t (t - \tau)^{[q] - q - 1} D^{[q]} x(\tau) d\tau.$$

For $[q] \in \mathbb{N}$, $D^{[q]}$ becomes the standard differential operator of IO and for $q \in (0, 1)$, as considered in this paper, $D^{[q]} x = x'$.

With the above notations, the FO IDMDE system becomes

$$\begin{aligned} D_*^q x_1 &= x_2 x_3 - x_1, \\ D_*^q x_2 &= (x_3 - p)x_1 - x_2, \quad x(0) = x_0, \\ D_*^q x_3 &= 1 - x_1 x_2, \end{aligned} \tag{3}$$

with $q \in (0, 1)$ and $p \in \mathbb{R}^+$.

The deeper numerical and theoretical analysis of the FO system (3) made in this paper reveals more interesting dynamics than those presented in [2], for example: the pure complex conjugated eigenvalues of equilibria indicate the use of center manifold approach, while attractors coexistence phenomenon leads to the existence of chaotic hidden attractors.

3 Equilibria

Equilibria, the two real solutions of the parametric equation $f(x) = 0$, $p \in \mathbb{R}^+$, are:

$$X_{1,2}^* = \left(\mp \frac{\sqrt{2}}{2} \sqrt{P+p}, \pm \frac{\sqrt{2}}{4} (p-P) \sqrt{P+p}, \frac{1}{2} (p+P) \right)$$

where

$$P := \sqrt{p^2 + 4}.$$

The Jacobian is

$$J(x) = \begin{bmatrix} -1 & x_3 & x_2 \\ x_3 - p & -1 & x_1 \\ -x_2 & -x_1 & 0 \end{bmatrix}.$$

Without restricting the generality, consider $p = 5$. Then, equilibria are

$$X_{1,2}^* (\mp 2.2787, \mp 0.4388, 5.1926),$$

and, for both equilibria, the eigenvalues are

$$\sigma_1 = -2, \quad \sigma_{2,3} = \pm 2.32053i.$$

The fact that $\text{Re}(\sigma_{2,3}) = 0$, suggests that $X_{1,2}^*$ should be analyzed via center manifold theory. However, Matignon Theorem for autonomous FO systems [23] can still be applied to determine the stability of $X_{1,2}^*$. Therefore, the following result can be proved

Theorem 1. *For $p = 5$, equilibria $X_{1,2}$ are asymptotically stable for $q \in (0, 1)$.*

Proof. Denote with

$$\iota = q - 2 \frac{|\alpha_{min}|}{\pi}, \tag{4}$$

where α_{min} stands as the minimum of the arguments of eigenvalues. As stated by the stability theorem [23], the considered equilibrium is asymptotically stable if $\iota < 0$, otherwise it is unstable. For $p = 5$, the arguments of the eigenvalues are $\alpha_1 = \pi$, $\alpha_{2,3} = \pm\pi/2$ and $|\alpha_{min}| = \pi/2$. Then

$$\iota = q - 1 < 0, \quad \text{for } q \in (0, 1),$$

and, therefore, equilibria $X_{1,2}$ are asymptotically stable. \square

Because, for the general case of $p \in [p_{min}, p_{max}]$, with $p_{min, max} > 0$, the explicit form of eigenvalues is too complicated to be presented here, let the following conjecture sustained by computation evidence according to which the stability result Theorem 1 is true for all considered values of p .

Conjecture 2. *Equilibria $X_{1,2}^*$ are asymptotically stable for $q \in (0, 1)$ and all $p > 0$.*

Numerical proof.

Consider lattice $L = \{(p, q) | p \in [p_{min}, p_{max}], q \in (0, 1)\}$ with $p_{min} = 0$ and $p_{max} = 10$. Then, exploring L with a finite relative small step, following the reasoning in Theorem 1 and using the symbolic calculus to determine the spectrum of the eigenvalues at every grid point $(p, q) \in L$, one can obtain ι with relation (4) which determines a two parametric surface in the space (p, q, ι) , denoted by S (Fig. 1 (a)). Note that for every q one eigenvalue is real constant: $\sigma_1 = -2$, while the other two are complex conjugate with $\text{Re}(\sigma_{2,3}) = 0$ (Fig. 1 (b)). As can be seen in Fig. 1 (a), the graph of S is situated under the horizontal critical plane Δ ($\iota = 0$), for $q \in (0, 1)$ and all values of p , which means that all points of S have coordinate ι negative. Moreover, from Fig. 1 (a) one deduces that for every fixed value of $q \in (0, 1)$, ι does not depend on $p \in [p_{min}, p_{max}]$. Therefore, for $q \in (0, 1)$, $X_{1,2}^*$ are stable for all considered values of p . \square

Note that the surface S crosses the plane $\iota = 0$ for $q = 1$ (case not considered in this paper), the stability of $X_{1,2}^*$ being critical.

Proposition 3. *For all considered p , the system (2) is dissipative.*

Proof. The generalized divergence $\nabla(f(x)) = \text{Tr}(J(x)) = -2 < 0$ and not depending on p . Therefore, the system is dissipative for all p . \square

To note that the dissipativeness could be useful to study the rapport between the absorbed and supplied energy of the system.

Remark 4. *i) Since $\text{Real}(\sigma_{2,3}) = 0$, in the IO variant of the system (2), the stability of equilibria $X_{1,2}^*$ cannot be studied via the known negativeness criterion of real components of eigenvalues and the stability has to be analyzed via center manifold theory. However, it is difficult to get the analytical expression of the centre manifold, but there are methods of the construction or approximation of center manifold (see e.g. [24]). A useful web service which constructs center manifolds for autonomous IO systems with general linearisation is [25];*

ii) The existence of center manifolds and its approximation for autonomous FO systems defined with Caputo's derivative, is studied in [26] and the center manifold of the Lorenz system of FO is calculated in [27].

ii) Related to Conjecture 2 and Proposition 3, it is worth noting that for IO systems, in [28,29] the instability condition of a point x , $\nabla f(x) > 0$, is considered (see also [30]). Let consider here the FO variant of divergence, which in our case, when $f = (f_1, f_2, f_3)^T$ and $x = (x_1, x_2, x_3)$, has the form [31]

$$\nabla^q f(x) = D_{*x_1}^q f_1(x_1, x_2, x_3) + D_{*x_2}^q f_2(x_1, x_2, x_3) + D_{*x_3}^q f_3(x_1, x_2, x_3),$$

where $D_{*x}^q := \frac{\partial^q}{\partial x^q}$ represents the partial Caputo's derivative with respect x . D_*^q being a linear operator, if $D_*^q f(x)$ and $D_*^q g(x)$ exist, then for $a, b \in \mathbb{R}$ one has

$$D_*^q(af(x) + bg(x)) = aD_*^q f(x) + bD_*^q g(x),$$

and also

$$D_*^q x^n = \frac{\Gamma(n+1)}{\Gamma(n-q+1)} x^{n-q}, \quad \text{for } n \in \mathbb{Z}^+ \quad \text{and } D_*^q \text{const} = 0.$$

Therefore, for $q \in (0, 1)$ and $p \in [p_{min}, p_{max}]$, within a rectangular planar domain (x_1, x_2) which contains the coordinates x_1^* and x_2^* of equilibria $X_{1,2}^*$ (since f_3 does not depend on x_3 , $\frac{\partial^q}{\partial x_3^q} f_3(x_1, x_2) = 0$, and $\nabla^q f(x)$ also does not depend on x_3), one has

$$\nabla^q f(x) = -\frac{\Gamma(2)}{\Gamma(2-q)} (x_1^{1-q} + x_2^{1-q}) < 0, \quad \text{for } q \in (0, 1).$$

In Fig.2, $\nabla^q f(x)$ is determined as function of x_1 and x_2 , for $q = 0.995$.

4 Local Lyapunov exponents

While for a given system “global” Lyapunov Exponents (LEs) offer information about the average growth of small perturbations, finite-time (or local) LEs provide “local” growth rates along a finite-time section of the trajectory and reveal the separation between trajectories. In this paper, finite-time LEs are considered.

Consider the general FO initial value problem (2) with $f : \mathbb{R}^n \rightarrow \mathbb{R}^n$ a smooth function. Then, there exists the time-variant variational system associated to (2) is the following linear FO system [32]

$$\begin{aligned} D_*^q \Phi(t) &= J(t)\Phi(t), \\ \Phi(0) &= I_n, \end{aligned} \tag{5}$$

where $\Phi \in \mathbb{R}^{n \times n}$ is the fundamental solution to (5) and $J(t)$ is the $n \times n$ Jacobian of f evaluated at the point $x(t)$, solution of (2), i.e. along the trajectory of the system (2).

The following existence result can be enounced (the proof can be found in [34])

Theorem 5. *The LEs are defined by the eigenvalues of the fundamental solution Φ obtained by solving the following combined (extended) system*

$$\left\{ \begin{array}{l} D_*^q x(t) \\ D_*^q \Phi(t) \end{array} \right\} = \left\{ \begin{array}{l} f(x(t)) \\ J(t) \cdot \Phi(t) \end{array} \right\}, \quad \left\{ \begin{array}{l} x(0) \\ \Phi(0) \end{array} \right\} = \left\{ \begin{array}{l} x_0 \\ I_n \end{array} \right\}. \tag{6}$$

The explicit form of (6) allows the numerical determination of LEs by using some numerical scheme for FDEs. Simultaneously with the integration of the system (3) (first equation of the extended system (6)), one integrate the second (variational) system in (6), where the solution of the first system is used. To obtain LEs, in this paper the Matlab code FO_Lyapunov for commensurate FO systems [33, 34] is utilized (for non-commensurate case see [35, 36]).

The code adapts the Benettin procedure [37] based on Multiplicative Ergodic Theorem of Oseledec [38] and using the Gram-Schmidt orthogonalization procedure to FO systems [34]. Despite the low efficacy and high sensitivity on algorithm parameters, and the potential loss of orthogonality, which all might lead to inaccurate numerical results, the algorithm proposed by Benettin remains one of most used numerical algorithms for IO LEs and seems to be useful for FO LEs too.

For the numerical integration consider the discretization of the time-integration interval $I = [0, T]$, $T > 0$, on which the numerical solution is determined, with grid points of some equidistant partition of I , $t_i = hi$, $i = 0, 1, 2, \dots, N$, where h is a fixed step size, $h = T/N$. With these ingredients in this manuscript one considers the known predictor-corrector method Adams-Bashforth-Moulton (ABM) for FO systems [12]¹.

In this paper the LEs along of a chaotic trajectory are determined (for the stable attractors $X_{1,2}^*$, obviously, LEs are negative for all q and p). For this purpose, the maximum time integration interval is $[0, T]$, with $T = 1700$, the integration step size $h = 0.02$ and the one of the most important parameter, h_{norm} , in FO_Lyapunov representing the time moments when the Gram-Schmidt orthogonalization is applied [34], was chosen multiple of h . Compared to several other cases of FO systems where the FO_Lyapunov code has been applied, in this case the value of h_{norm} is relatively higher, but chosen together with h so as to be consistent: positive or negative values of LEs correspond, in the vast majority of cases, to chaotic or stable attractors, respectively.

As known, longer time integration intervals in the integration of IO systems could lead to wrong results (see e.g. [40, 41]). However, on the other side, this system presents chaotic transients sets which must be avoided (see e.g. the case $p = 1.2$ and $q = 0.995$ (point M in Fig. 3 (d)) for the initial condition $x_0 = (0.1, 0.1, 0.1)$, with the corresponding time series in Fig. 3 (e) where, after a chaotic transient which lasts at about $t = 1300$, the trajectory tends to the first coordinate of the stable equilibrium $X_1^*(-1.3290, -0.7525, 1.7662)$). Therefore, the intensive realized numerical experiments proved that the relative large time interval $[0, 1700]$, represents the best choice to overcome chaotic transients.

Due to these mentioned characteristics of the FO IDMDE system and to inherent numerical errors which characterizes the Benettin algorithm, amplified by the numerical errors introduced by the ABM method for FO systems, the results should be interpreted with caution. For this system and presented data, the observed errors of LEs are of order of $5e - 2$.

Denote by $\lambda_1, \lambda_2, \lambda_3$ with $|\lambda_1| < |\lambda_2| < |\lambda_3|$ the spectrum of the LEs. Because LEs depend on q and also on p , they can be plotted in the space (p, q, λ) as function of p and q (see Fig. 3 (a), where the most representative range for q , $q \in [0.98, 1)$ has been considered; for $q \in (0, 0.98)$ nothing dynamically interesting happens). To every λ_i , $i = 1, 2, 3$ it corresponds a surface denoted S_λ . In this way one can obtain a general view of LEs, not only as the usual representation as function of the parameter p , or as function of q . The surface S_{λ_2} (blue plot) is under the horizontal plane $\lambda = 0$ and close to it indicating the negativeness of λ_2 for all considered q and p . Similarly, S_{λ_1} (green plot) represents the negative values of λ_1 . The only surface presenting positive values (red plot) is S_{λ_3} .

As expected, the LEs along trajectories leading to equilibria $X_{1,2}^*$ are all negative and are

¹A fast Matlab implementation can be found at [39].

not considered here.

Remark 6. *In the combined system (6), $x(t)$ stands as the current state of the trajectory of the underlying system (3), used to find Φ and, therefore, the initial condition x_0 should be chosen inside the basin of attraction of the studied attractor (here chaotic) otherwise, wrong results might be obtained. As known, if p or q are varied while (6) is integrated, the attraction basin might change and, therefore, the reference trajectory calculated by the algorithm for LEs could “jump” to another trajectory leading to wrong LEs (see the switched between positive (corresponding to the chaotic attractor) and negative or zero values (corresponding to the stable equilibria $X_{1,2}^*$) in Fig. 3 (b) and (c) which, by the mentioned reasons, couldn’t be avoided). For the simulations utilized in this paper to obtain the LEs, the utilized initial conditions are $x_0 = (1e-3, 1e-3, 1e-3)$ (note that other initial conditions could enter other attraction basins, see Fig. 3 (e) where the trajectory is obtained with the initial condition $x_0 = (0.1, 0.1, 0.1)$).*

5 Chaotic hidden attractor

Considering that the positiveness of at least one LE ensures the existence of chaos², one can see that the chaotic attractor, exists only for a relative small domain in the plane (p, q) (see the surface S_{λ_3} (red plot), situated above the plane $\lambda = 0$ in Fig. 3 (a) and also the projection of this positive part of S_{λ_3} on the plane (p, q) , denoted B_{HA} , in Fig. 3 (d), which can be considered as an attraction parametric basin-like). Beside the parameters (p, q) which generate chaotic dynamics, B_{HA} also allows the determination of minimum value of q for which chaos is enhanced, namely a value nearly 0.988.

Summarising the results on LEs (Section 4), from Figs. 3 (a) and (d), the following important property of the FO system (3) can be enounced

Proposition 7. *For all considered values of $p \in [0, 10]$, there exists $q \in (0, 1)$ for which the system (2) behaves chaotic. Moreover, for q close to 1, the system is chaotic for all p .*

If one intersect the surfaces S_{λ_i} , $i = 1, 2, 3$, with an orthogonal plane to the plane (p, q) and parallel with the plane (p, λ) , the intersection curves indicate the evolution of λ_i , $i = 1, 2, 3$ as function on p (see plane Π through $q = 0.995$ in Fig. 3 (a)). Similarly, one can obtain the evolution of LEs, for some fixed value p , as function of q , if one intersect an orthogonal plane parallel to the plane (q, λ) (see plane Δ through $p = 8$ in Fig. 3 (a)). In Fig 2 (b) the variation of the maximal LE, λ_3 , as function of p , determined for $q = 0.995$, λ_3 , is consistent with the intersection of S_{λ_3} with the plane Π . Fig. 3 (c) represents the evolution of the maximal LE, λ_3 , for $p = 5$, as function of q .

Definition 8. *[19, 20] An attractor is called a hidden attractor if its basin of attraction does not intersect with a certain open neighbourhood of equilibrium points; otherwise it is called a self-excited attractor.*

²It is possible to construct examples in which the system has positive Lyapunov exponents along a zero solution of the original system but, at the same time, this zero solution of original nonlinear system is Lyapunov stable (Perron’s effect [42], see also [43]).

Following the stability of equilibria $X_{1,2}^*$ (Conjecture 2), and also due the existence of an chaotic attractor (Proposition 7), the following result can be established

Proposition 9. *The chaotic attractor of the system (2) is hidden.*

Proof. Following Definition 8, the proof is obvious since $X_{1,2}^*$ are asymptotically stable and attract trajectories starting from neighborhoods of $X_{1,2}^*$. \square

In Fig.4 is presented the chaotic hidden attractor (dark green plot), denoted HA, corresponding to $p = 5$ and $q = 0.995$.

To sustain numerically Proposition 9, let a two-dimensional representation of the attraction basin of HA corresponding to $p = 5$ and $q = 0.995$, consider the plane $\Sigma = \{(x_1, x_2, x_3^*) | x_1, x_2 \in \mathbb{R}, x_3^* = 5.1926\}$ which contains equilibria $X_{1,2}^*$ (Fig. 5 (a)). Because third coordinates of $X_{1,2}^*$, x_3^* , are identic Σ is horizontal and passes through $X_{1,2}^*$. In this plane a lattice of 100×100 points $(x_1, x_2, x_3^*) \in [-5, 5] \times [-5, 5] \times \{x_3^*\}$, is considered and at each of these points, considered as initial condition x_0 , the system (2) is integrated to determine where trajectories tend. Points which lead to equilibria $X_{1,2}^*$ are plotted blue (corresponding to X_1^*) or red (corresponding to X_2^*), while points which tend to the chaotic attractor are plotted light green. As can be seen, around equilibria there exists a relative large neighborhoods (with the disc in Fig. 5 (a)) which contain only points attracted by one of equilibria $X_{1,2}$ respectively³.

HA, plotted in Fig. 4, starts from the initial condition $x_0 = (-2.5, 4.5, x_3^*)$, $x_3^* = 5.1926$ (point 3 in Figs 5), but following the definition of an attractor, could be generated from any other “green” initial condition. The stable attractors $X_{1,2}^*$ (light blue and magenta plots), respectively, are reached from initial condition $x_0 = (4, 2.5, x_3^*)$ (point 1 in Figs 5) and initial condition $x_0 = (2.5, -3.5, x_3^*)$ (point 2 in Fig. 5). Similarly to the chaotic attractor HA, for the considered case, horizontal section through x_3^* , $X_{1,2}^*$ can be reached from any other “blue” or “red” initial condition.

In the parametric space, HA corresponds to the point R in Fig. 2 (d), having the corresponding maximum LE, λ_3 , marked by the black circles in Figs. 3 (b) and (c). As expected, for these values of p and q , the value of λ_3 is similar in both LE representations, $\lambda_3 \approx 2.1$.

As expected, Fig. 5 (b) shows that the chaotic HA crosses the horizontal plane through $x_3 = x_3^*$ only in light green points, which represent the attraction basin of HA, and not red or blue points which represent the attraction basins of $X_{1,2}^*$.

As can be seen in the crossing plane Σ (Fig. 5 (b)) the area of the attraction basin of HA is quite larger than the area of attraction basins of stable equilibria $X_{1,2}^*$, fact which suggests that the probability of the system to evolve chaotically for arbitrary initial conditions is quite large.

Conclusion

In this paper a novel IO system modelling the interaction between dark matter and dark energy has been considered in the general form of a fractional order system modeled by

³A three-dimensional representation of an attraction basin of chaotic hidden attractors is presented in [44].

Caputo's derivative. Its rich dynamics are estimated theoretically and numerically. Because the interaction between dark matter and dark energy affecting the cosmic structures is one of not completely solved problems in cosmology, the fractional approach as generalization of dynamics of integer order, could help the understanding of these dynamics such as the presence of chaos for total order less than 3, or the existence of hidden attractors. The system presents a center equilibria whose stability could be analyzed via Matignon criterion, not via the sign study of the real components of related eigenvalues. The numerical integration has been done with the ABM method for FO systems and the local Lyapunov exponents are found with the Matlab code FO_Lyapunov.m. Because the equilibria are asymptotically stable, the existing chaotic attractor is hidden. Further analysis of the FO system for larger values of the parameter p has to be realized.

Acknowledgement

Author thanks Abdullah Gokyildirim and Haris Calgan for verifying the existence of the chaotic HA by means of circuit implementations.

References

- [1] Rezaei Z. Dark Matter–Dark Energy Interaction and the Shape of Cosmic Voids. *The Astrophysical Journal* 2020;902(2):2020.
- [2] Aydiner E. Chaotic interactions between dark matter and dark energy, arXiv:2304.06614v1 [gr-qc] 13 Apr 2023
- [3] Aydiner E. Chaotic universe model. *Scientific REPOrts* — 2018;8:721
- [4] J. Sprott J. A proposed standard for the publication of new chaotic systems. *Int J Bifurcation Chaos* 2011;21(9):2391–2394.
- [5] Sprott J, Linz, S. Algebraically Simple Chaotic Flows. *Int J Chaos Theory Appl* 2000;5(2):1–20.
- [6] Oldham K, Spanier J. *The Fractional Calculus: Theory and Applications of Differentiation and Integration to Arbitrary Order*; Academic Press: New York, NY, USA,1974.
- [7] Podlubny I. Geometric and physical interpretation of fractional integration and fractional differentiation. *Fract Calc Appl Anal* 2002;5:367–386.
- [8] Ray SA, Atangana A, Noutchie SCO, Kurulay M, Bildik N, Kilicman A. Fractional calculus and its applications in applied mathematics and other sciences. *Math Probl Eng* 2014:849395.
- [9] Diaz JB, Olser TJ. Differences of fractional order. *Math Comput* 1974;28(125):185–202.
- [10] Almeida R. A Caputo fractional derivative of a function with respect to another function. *Communications in Nonlinear Science and Numerical Simulation* 2017;44:460–481.

- [11] Teodoro GS, Tenreiro Machado JA, Capelas de Oliveira E. A review of definitions of fractional derivatives and other operators. *Journal of Computational Physics* 2019;388:195–208.
- [12] Diethelm K, Ford NJ, Freed AD. A predictor-corrector approach for the numerical solution of fractional differential equations. *Nonlinear Dyn* 2002;29:3-22.
- [13] Danca Marius-F. Fractional order logistic map: Numerical approach, *Chaos, Solitons & Fractals* 2022;157:111851
- [14] Atici FM, Eloe PW. Initial value problems in discrete fractional calculus. *Proc Americ Math Soc* 2007;137:981–989
- [15] Abdeljawad T. On Riemann and Caputo fractional differences. *Computers & Mathematics with Applications* 2011;62(3):1602–1611.
- [16] Wu GC, Baleanu D, Zeng SD. Several fractional differences and their applications to discrete maps. *J Appl Nonlinear Dyn* 2015;4:339–348
- [17] Wu GC, Baleanu D, Xie HP, Chen FL., Chaos synchronization of fractional chaotic maps based on the stability condition. *Physica A* 2016;460:374–383.
- [18] Khennaoui AA, Ouannas A, Bendoukha S, Grassi G, Wang X, Pham VT, Alsaadi FE. Chaos, control, and synchronization in some fractional–order difference equations. *Advances in Difference Equations* 2019;412:2019–412
- [19] Leonov GA, Kuznetsov NV, Mokaev TN. Homoclinic orbits, and self-excited and hidden attractors in a Lorenz-like system describing convective fluid motion. *The European Physical Journal Special Topics* 2015;224 (8):1421–1458.
- [20] Leonov GA, Kuznetsov NV. Hidden attractors in dynamical systems. From hidden oscillations in Hilbert-Kolmogorov, Aizerman, and Kalman problems to hidden chaotic attractor in Chua circuits. *Int J Bifurcation Chaos* 2013; 23 (1):1330002–219.
- [21] Dudkowski D, Jafari S, Kapitaniak T, Kuznetsov NV, Leonov GA, Prasad A. Hidden attractors in dynamical systems. *Physics Reports* 2016;637:1-50,
- [22] Andrievsky BR, Kuznetsov NV, Leonov GA, Pogromsky AY. Hidden oscillations in aircraft flight control system with input saturation. *IFAC Proceedings Volumes (IFAC-PapersOnline)* 2013;46(12):75-79.
- [23] Matignon D. Stability properties for generalized fractional differential systems, in *Proceedings of the Fractional Differential Systems: Models, Methods and Applications* 1998:145–158.
- [24] https://en.wikipedia.org/wiki/Center_manifold
- [25] <http://www.maths.adelaide.edu.au/anthony.roberts/gencm.php>

- [26] Ma L, Li C. Center Manifold of Fractional Dynamical System. *Journal of Computational and Nonlinear Dynamics*, 2016;11:021010-1
- [27] Guo Y, Sun Y. Centre Manifold of Fractional-order Lorenz system, *Proceedings of 2017 the 7th International Workshop on Computer Science and Engineering (WCSE 2017)* Beijing, 25-27 June, 2017, pp. 326-330, doi: 10.18178/wcse.2017.06.056.
- [28] Zhukov VP. On one method for qualitative study of nonlinear system stability. *Automat Rem Contr+* 1978;39(6), 785-788 (in Russian).
- [29] Zhukov VP. On the method of sources for studying the stability of nonlinear systems. *Automat Rem Contr+* 1979;40(3), 330-335 (in Russian)
- [30] Furtat I, Gushchin P, Nekhoroshikh A. Divergence Conditions for Stability Study of Autonomous Nonlinear Systems. *IFAC PapersOnLine* 2020;53-2:6317–6320.
- [31] Danca MF. Hopfield Neuronal Network of Fractional Order: A note on its numerical integration. *Chaos, Solitons & Fractals* 2021;151:111219.
- [32] Li C, Gong Z, Qian D, Chen YQ. On the bound of the Lyapunov exponents for the fractional differential systems, *CHAOS* 2010;20:013127.
- [33] <https://www.mathworks.com/matlabcentral/fileexchange/114595-matlab-code-for-lyapunov-exponents-of-fractional-order>
- [34] Danca Marius-F. Nikolay Kuznetsov, Matlab code for Lyapunov exponents of fractional order systems. *Int J Bifurcation Chaos* 2018;28(05):1850067.
- [35] Danca Marius.-F. Matlab code for Lyapunov exponents of fractional-order systems, Part II: The non-commensurate case. *Int J Bifurcation Chaos* 2021;31(12):2150187.
- [36] <https://www.mathworks.com/matlabcentral/fileexchange/122377-matlab-code-for-les-of-non-commensurate-fo>
- [37] Benettin G, Galgani L, Giorgilli A, Strelcyn J-M. Lyapunov characteristic exponents for smooth dynamical systems and for hamiltonian systems. A method for computing all of them. Part II: Numerical application. *Meccanica* 1980;15:21–30.
- [38] Oseledets V I. A multiplicative ergodic theorem. Characteristic Ljapunov, exponents of dynamical systems. *Trudy Moskov Mat Obšč* 1968;19:179–210.
- [39] <https://www.mathworks.com/matlabcentral/fileexchange/32918-predictor-corrector-pece-method-for-fractional-differential-equations>
- [40] ShiJun Liao, PengFei Wang, On the mathematically reliable long-term simulation of chaotic solutions of Lorenz equation in the interval $[0,10000]$. *Science China Physics, Mechanics and Astronomy* volume 2014;57:330–335.

- [41] Scott AS, Clyde M. On the numerical solution of chaotic dynamical systems using extend precision floating point arithmetic and very high order numerical methods. *Nonlinear Analysis: Modelling and Control*, 2011;16(3):340–352.
- [42] Kuznetsov NV, Leonov GA. On stability by the first approximation for discrete systems. *Proceedings. 2005 International Conference Physics and Control, 2005. Vol. Proceedings Volume 2005.* pp. 596–599.
- [43] https://en.wikipedia.org/wiki/Lyapunov_exponent
- [44] Danca Marius-F, Bourke P, Kuznetsov N. Graphical structure of attraction basins of hidden attractors: the Rabinovich-Fabrikant system. *Int J Bifurcation Chaos* 2019;29(01):1930001.
- [45] Diaz JB, Olser TJ. Differences of fractional order. *Math Comput* 1974;28(125):185–202.

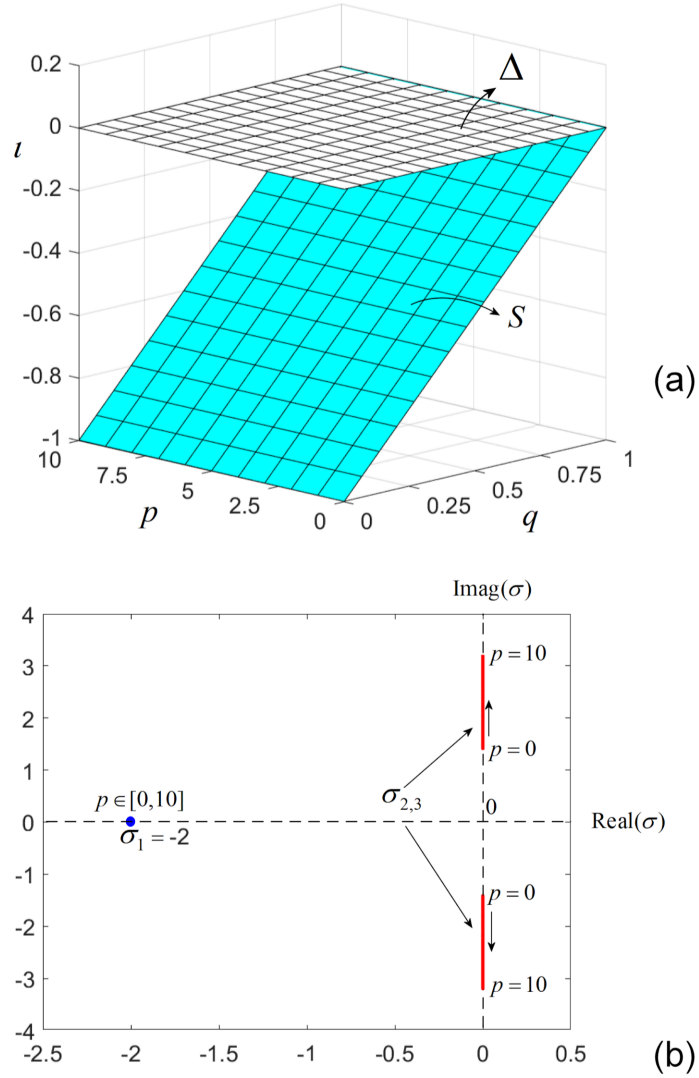


Figure 1: Stability of equilibria $X_{1,2}^*$. (a) Graph S generated by ι (4) as function of p and q (light blue); (b) Eigenvalues plot as function of p : the real eigenvalue $\sigma_1 = -2$ (blue plot), and the pure complex conjugate eigenvalues $\sigma_{2,3}$ (red plot) for $p \in [0, 10]$.

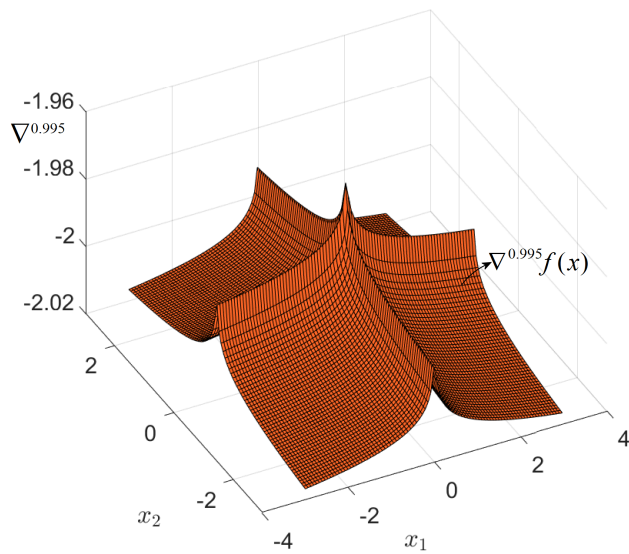


Figure 2: Graph of the fractional divergence $\nabla^{0.995} f(x)$.

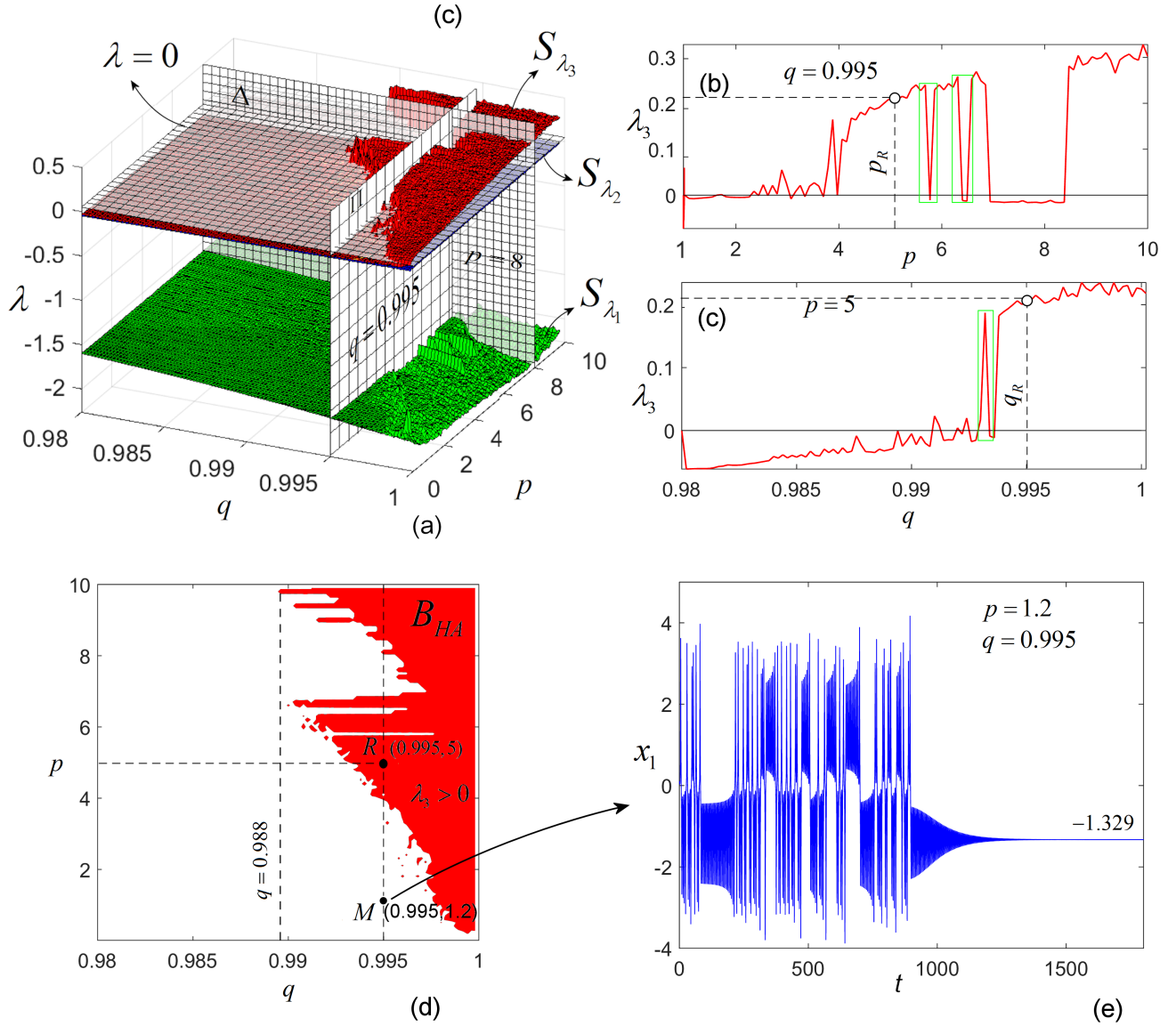


Figure 3: Local LEs. (a) Surfaces S_{λ_i} , $i = 1, 2, 3$, determined by LEs, plotted as function of p and q ; (b) Evolution of the maximum LE, λ_3 , as function of p for $q = 0.995$ (see Fig. 3 (d) for p_R); (c) Graph of the maximum LE, λ_3 , as function of q for $p = 5$ (see Fig. 3 (d) for q_R); (d) Projection on the plane (p, q) of the positive surface S_{λ_3} (red plot), denoted B_{HA} ; (e) Time series of a relative longue chaotic transient corresponding to $p = 1.2$, $q = 0.995$ corresponding to point M in Fig. 3 (d) for the initial condition $(0.1, 0.1, 0.1)$.

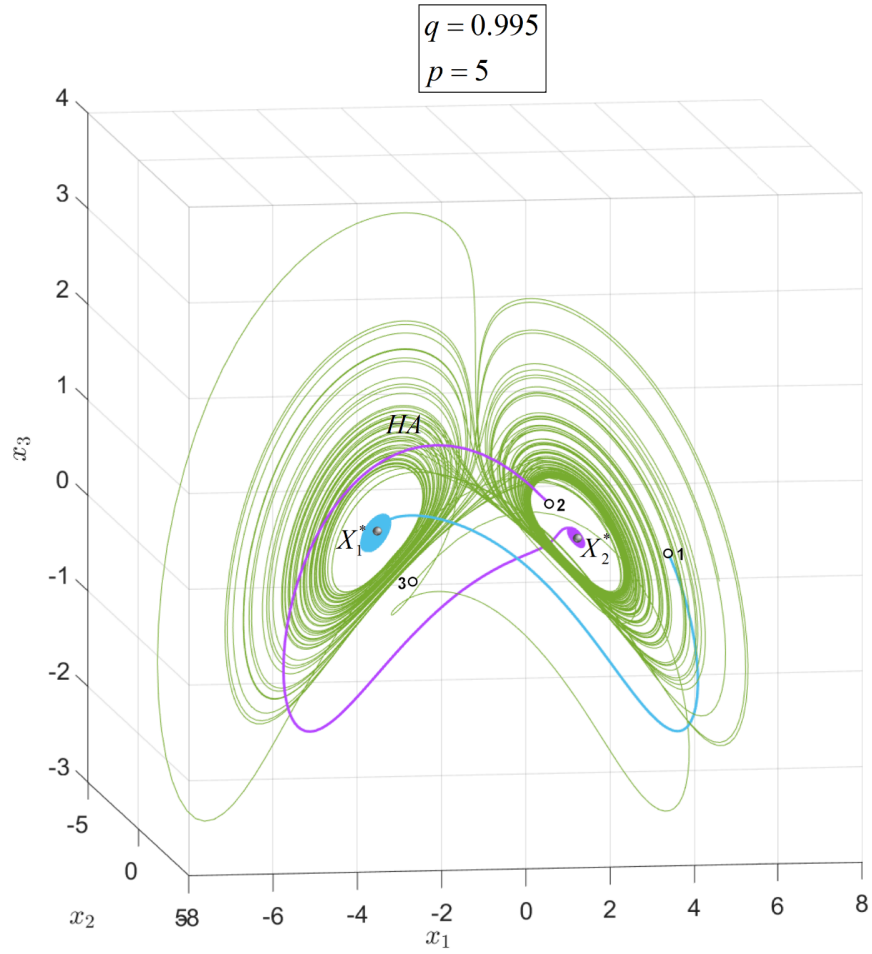


Figure 4: The chaotic hidden attractor, HA (dark green plot), and the stable equilibria $X_{1,2}^*$ (magenta plot) for $p = 5$ and $q = 0.995$.

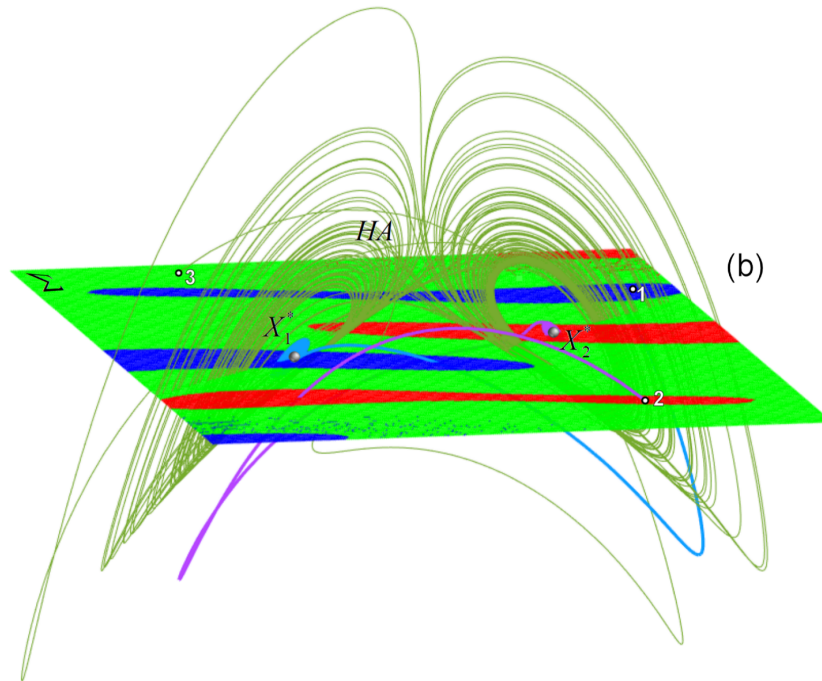
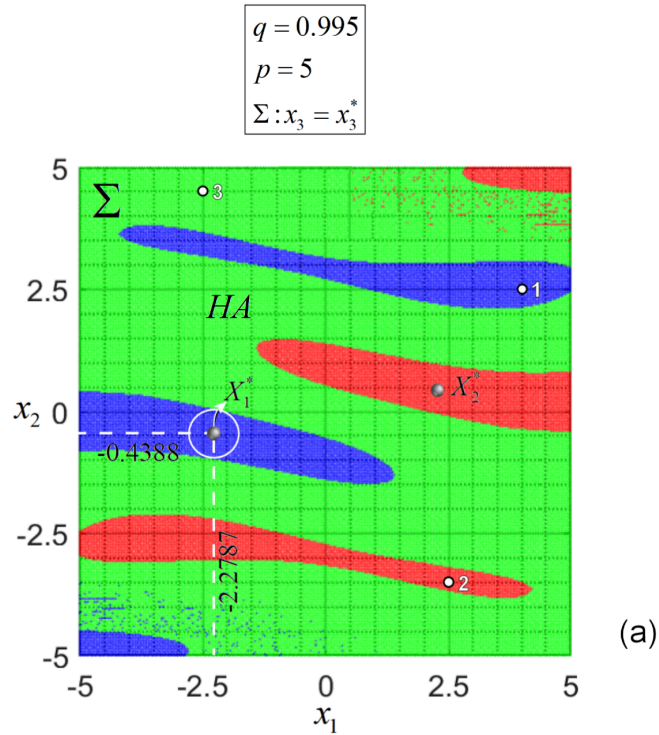


Figure 5: Attraction basin of the chaotic HA for $p = 5$ and $q = 0.995$. (a) Horizontal intersection Σ of the attraction basin of the chaotic HA, with the plane $x_3 = x_3^*$, containing equilibria $X_{1,2}^*$. Blue points are attracted by the equilibrium X_1^* , red points by the equilibrium X_2^* , while green points represent the initial conditions in the plane $x_3 = x_3^*$ leading to HA; (b) The trajectory generating the chaotic HA (dark green plot) crosses Σ only on light green points. Points denoted 1,2 and 3 represent the initial conditions x_0 used to generate trajectories tending to X_1^* , X_2^* and HA, respectively (see also Fig. 5 (a)).